Microchimica Acta (2019) 186: 633
https://doi.org/10.1007/s00604-019-3706-0

ORIGINAL PAPER

Cysteine-assisted photoelectrochemical immunoassay for the carcinoembryonic antigen by using an ITO electrode modified with C_3N_4-BiOCl semiconductor and CuO nanoparticles as antibody labels

Bing Zhang[1] · Yejing Jia[1] · Jing Wang[1] · Xing Hu[1] · Zhihuan Zhao[1] · Yan Cheng[2]

Received: 22 March 2019 / Accepted: 21 July 2019 / Published online: 18 August 2019

Abstract

A sensitive photoelectrochemical (PEC) immunoassay for the carcinoembryonic antigen (CEA) is described that is based on the use of C_3N_4-BiOCl semiconductor on an ITO electrode. The photocurrent of the modified electrode was measured under visible light illumination. It increased in presence of L-cysteine due to rapid separation of the photoexcited electrons and holes. A sandwich-type immunoassay in a 96-well microtiter plate format used CuO nanoparticles as label for the secondary antibody. The Cu^{2+} is released from the CuO in the sandwich complex by treatment with acid. The free Cu^{2+} combined with both the cysteine and the electron receptors of C_3N_4 and BiOCl. Under optimal conditions, this dual action immensely decreases the photocurrent of the PEC system, and the response is inversely proportional to the CEA concentrations from 0.1 pg mL^{-1} to 10 ng mL^{-1} at the working voltage of 0 V (vs. SCE). The detection limit is 0.1 pg mL^{-1}, and the method is exhibited satisfactory selective, repeatable and stable.

Keywords Sandwich immunoassay · Tumor marker · Two-dimension nanomaterials · Cu^{2+}

Introduction

The detection of tumor markers plays an indispensable role in early discovery and diagnosis for malignant tumor [1]. Immunoassays for tumor markers depend on various analytical techniques, such as ELISA [2], chemiluminescent [3], photoelectrochemical [4], electrochemical [5], fluorescence [6], colorimetric [7] and so on. Photoelectrochemical immunoassay as a powerful and promising technology has gained more and more attention, concerning with the interaction of light and electrochemical systems [8, 9]. The high sensitivity is obtained for photoelectrochemical immunoassay due to the mutual independence of excitation signal (light) and detection signal (electricity) [10].

The photoelectrochemical conversion requires a semiconductor to absorb light and generate electron-hole pairs, which play an important role for constructing photoelectrochemical platform. Photocatalyst semiconductor can accelerate the photoreaction and enhance the kinetics of electron transfer. Varieties of photocatalysts are developed including TiO_2, CdS, C_3N_4, $BiVO_4$, Ta_3N_5, Bi_2S_3, WS_2 and so on [11–16]. Different kinds of photocatalysts are applied into the field of water splitting, hydrogen production, biosensing, solar cell and so on [17]. For wide band gap semiconductor, high energy source (particularly ultraviolet light) is usually required to excite them to generate photocurrent. To make full use of the sunlight, more research has focused on visible-light photocatalyst such as CdS, MoS_2, C_3N_4, BiOCl and so on [18–21]. Among graphitic carbon nitride (g-C_3N_4) as metal-free photocatalyst has obtained more and more attention because of its narrow band gap and feasible preparation [22]. However, the photocatalytic performances of g-C_3N_4

Electronic supplementary material The online version of this article (https://doi.org/10.1007/s00604-019-3706-0) contains supplementary material, which is available to authorized users.

✉ Bing Zhang
zhangbing01@tyut.edu.cn

✉ Yan Cheng
chengyan_1976@163.com

[1] College of Biomedical Engineering, Taiyuan University of Technology, Taiyuan 030024, China

[2] Department of Nuclear Medicine, First hospital of Shanxi Medical University, Taiyuan 030001, China

are limited due to its rapid recombination rate of photo-induced carriers.

To overcome this limitation and improve the photocatalytic activity, different modification methods for g-C_3N_4 including doping of metal or nonmetal elemental, combination of narrow band or wide band semiconductor and introduction of co-catalysts have been exploited. And heterojunctions structure of C_3N_4 with other semiconductor such as $NiTiO_3$, Bi_4NbO_8Cl, Cu_3P, MnO_2 and so on can accelerate the separation of photo-induced carriers due to mutual contaction of two semiconductors [23–26]. For example, Zhong et al. constructed CdSe quantum dots/g-C_3N_4, which showed remarkably intensive photocatalytic activity for visible-light-induced H_2 evolution because of its excellent visible absorption and high charge separation efficiency [27]. Zhang et al. reported SnO_2/SnS_2/C_3N_4 nanocomposites exhibited intense PEC signal responses compared with each single component, which were utilized for building PEC immunoassay [28]. And sacrificial donor such as ethanol, H_2O_2, ascorbic acid, cysteine also can enhanced photocatalytic activity through oxidation of sacrificial donor. For example, Manwar et al. used ethanol as a sacrificial donor to enhance photocatalytic hydrogen evolution [29].

Herein, C_3N_4-BiOCl semiconductor was prepared to construct photoelectrochemical sensing by photovoltaic conversion. And we explored L-cysteine as sacrificial donor to assist photoelectrochemical reaction and enhanced the photocurrent response. Sandwich-type immunoassay was constructed on 96-well microtiter plate based on CuO nanoparticles as labels. The released Cu^{2+} ions from CuO nanoparticles can weaken the photocurrents of C_3N_4-BiOCl by chelate with cysteine and as the electron receptors. And the low-abundant CEA biomarker (as a model) was quantitatively detected based on this new photoelectrochemical immunoassay system.

Experimental

Chemicals

CEA antigen with various concentrations (D620003–0100), 96-well microtiter plate and polyclonal CEA antibody (D120003–0025, Ab2, 0.01 mg mL^{-1}) were purchased from Sangon Biotech. Co., Ltd. (Shanghai, China, http://www.sangon.com/). L-cysteine (L-Cys), bismuth nitrate pentahydrate ($Bi(NO_3)_3{\cdot}5H_2O$), melamine, copper acetate ($Cu(AC)_2$), bovine serum albumin (BSA) and polydiallyldimethylammonium chloride (PDDA) were purchased from Aladdin Reagent Company (Shanghai, China, http://www.aladdin-e.com/). The 0.2 M phosphate buffer at various pH values were prepared by mixing the stock solutions of 0.2 M NaH_2PO_4, 0.2 M Na_2HPO_4 and 0.2 M KCl with different proportion. All the other chemicals were of analytical reagents grade and used without further purification. Clinical patient's serum samples were made available by first hospital of Shanxi medical university.

Synthesis of the C_3N_4-BiOCl semiconductor

Initially, carboxylated g-C_3N_4 was synthesized completely according to our previously reported method [30]. First, melamine powder (5.0 g) was calcined at 550 °C for 4 h in air. And the yellow g-C_3N_4 powder was collected by grinding at room temperature. To get the carboxyl group, the prepared g-C_3N_4 powder was refluxed in HNO_3 (100 mL, 5 M) for 24 h at 125 °C. Cooling to room temperature (RT, 25 ± 0.5 °C), the product was adjusted to pH 7.0 by centrifugation and cleanse with double distilled water. The final product was dried at 60 °C in a vacuum drying oven for 12 h to obtain carboxylate g-C_3N_4.

After, 0.30 g of g-C_3N_4 powder dispersed into water (25 mL) by ultrasound for 30 min to form suspension. Subsequently, bismuth nitrate pentahydrate (0.49 g), polyvinyl pyrrolidone (0.40 g) and glycerol (25 mL) were added into above solution and the mixed solution stirred vigorously for 1 h at RT. Then, 5 mL of saturated NaCl solution was dropwise added into this mixture solution and stirred for other 1 h. Then the hydrothermal reaction was carried out at 160 °C for 6 h in high pressure reactor. Finally, the product was collected by centrifugation and wash with double distilled water, which designed as C_3N_4-BiOCl.

Synthesis of CuO nanoparticles and bioconjugates

50 mL of ethanol mixture containing $Cu(Ac)_2$ (1 mM) and HAc (2 mM) was refluxed at 78 °C. Then, 5 mL of NaOH solution (4 mM) was dropwise added into the solution under vigorous stirring and reacted for 1 h. And CuO NPs formed by the alcohothermal method [31]. Then the suspension was centrifuged and washed three times with deionized water. The CuO powder was collected by drying at 60 °C. To get CuO-antibody conjugates, 1 mg of CuO NPs dispersed into 1 mL of phosphate buffer (0.2 M, pH 7.4) and sonicated for 10 min. Then, 500 μL of CEA polyclonal antibody was added into the CuO NPs solution. The mixture was transferred into refrigerator and incubated overnight at 4 °C. After centrifugation and washing, the CuO-Ab2 conjugates were collected and re-dispersed in 1 mL of phosphate buffer (pH 7.4) for further use. To block nonspecific bonding sites, the CuO-Ab2 dispersion incubated with BSA (0.5%) for 30 min at room temperature. Finally, the CuO-Ab2 conjugates were collected by centrifugation and washing.

Immunoassay protocol

The sandwich-type immunocomplex was constructed on 96-well microtiter plate. First, a 96-well plate was coated with 100 μL of CEA (10 μg mL^{-1}) in phosphate buffer (pH = 7.4) and incubated overnight at 4 °C. After washing with phosphate buffer three times, 200 μL of BSA (10%) blocking phosphate buffer was added into each well and incubated for 2 h at RT. Finally, the 96-well plate stored at 4 °C for further use after washing three times with phosphate buffer. CEA antigen (50 μL) were added into the 96-well plate and incubated for 70 min at RT. Afterwards, the 96-well plate was washed three times with ultrapure water to remove dissociative CEA. Then, 50 μL of CuO-Ab2 bioconjugates was added into the microplate and incubated for another 70 min. After washing three times, 200 μL of HNO_3 (0.1 M) was added into the 96-well plate to release Cu^{2+} from the CuO nanolabels. Subsequently, the Cu^{2+} solution was transferred into PEC test cell. The preparation process and principle of the immunoassay was described in Scheme 1a.

Photoelectrochemical measurements

The photoelectrochemical measurements were carried out in CHI660E (Chenhua, Shanghai, China) with xenon lamp. First, the bare ITO electrodes were thoroughly sonicated in ethanol/NaOH, acetone and distilled water for 10 min respectively, and dried at RT. Thereafter, 20 μL of C_3N_4-BiOCl (2 mg mL^{-1}) was carefully cast to electrode surface after 1% of PDDA (20 μL) formed in the surface of ITO (designed as C_3N_4-BiOCl/PDDA/ITO). For PEC detection, the C_3N_4-BiOCl/PDDA/ITO was inserted into phosphate buffer containing L-Cys and copper ions. And photocurrents were obtained in the three-electrode system with working voltage of 0 V.

Results and discussion

Characterizations of C_3N_4-BiOCl and CuO

Transmission electron microscope (TEM), X-ray powder diffraction (XRD), FTIR spectra, UV-vis diffuse reflectance spectra (DRS) of C_3N_4-BiOCl and transmission electron microscope (TEM), UV-vis absorbance spectra of CuO NPs are described in detail in ESM (Fig. S1 and Fig. S2).

Mechanism of photoelectrochemical assay

C_3N_4-BiOCl semiconductor showed excellent photoelectric conversion ability. To highlight this advantage, the photocurrent responses of different semiconductor were measured under visible light irradiation. As plotted in Fig. 1a, C_3N_4-BiOCl (curve *'d'*) shows highest photocurrent intensity compared with that of C_3N_4 (curve *'b'*) and BiOCl (curve *'c'*). The result attributed to the interfacial transition of photoexcited charge-carrier, which was proved by photoluminescence (PL) spectrometry. As shown in Fig. 1b, the PL spectrum was obtained at an excitation wavelength of 370 nm. C_3N_4-BiOCl (curve *'b'*) shows weak PL emission intensity compared with that of pure g-C_3N_4 sample (curve *'a'*). Those results showed C_3N_4-BiOCl hybrids can greatly suppress the recombination of photoexcited charge-carrier.

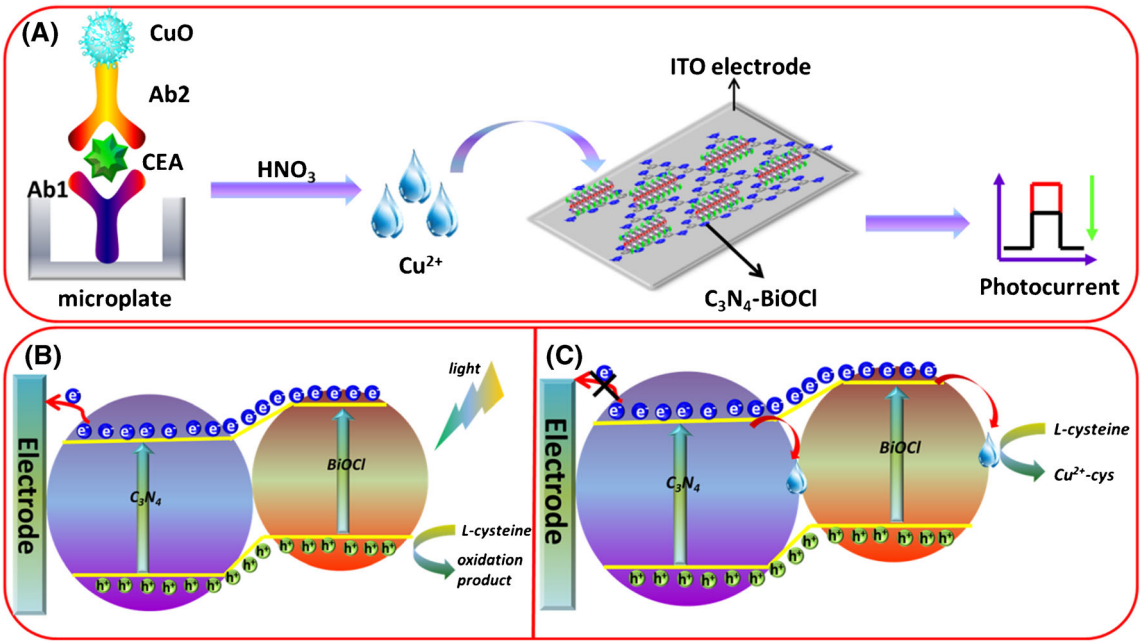

Scheme 1 **a** Schematic illustration of photoelectrochemical immunoassay; **b** Principle of photoelectric conversion of C_3N_4-BiOCl; and (**c**) Mechanism of Cu^{2+}-quenched photocurrent of C_3N_4-BiOCl containing L-cys

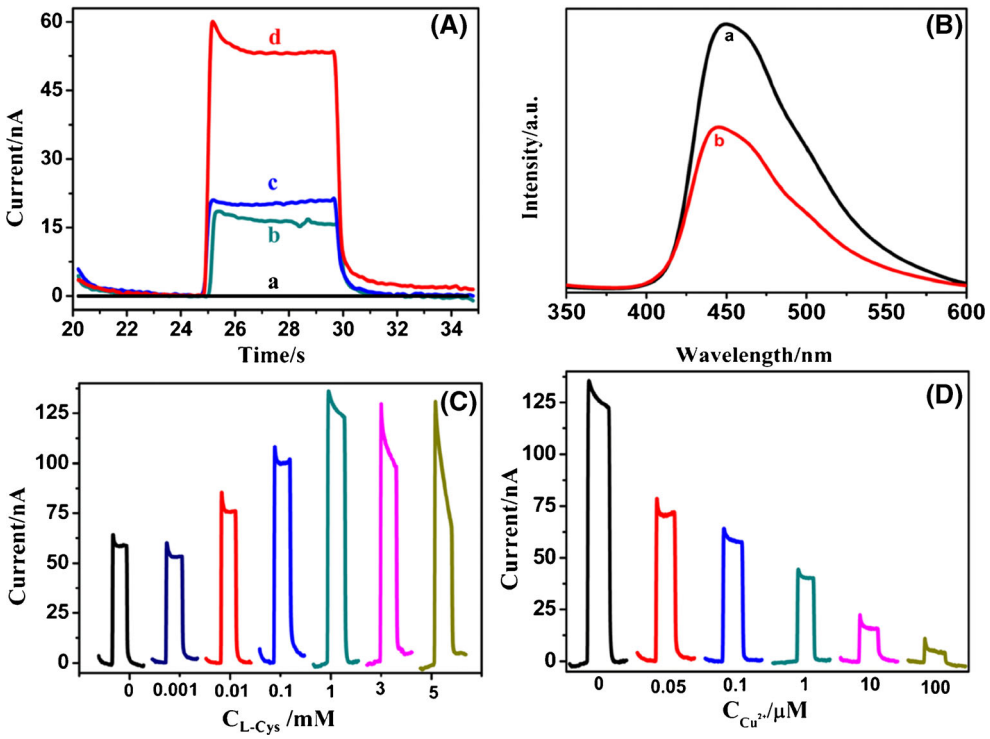

Fig. 1 **a** Photocurrents of (a) bare ITO electrode, (b) BiOCl/ITO, (c) C_3N_4/ITO, (d) C_3N_4-BiOCl/ITO in phosphate buffer; **b** PL of (a) C_3N_4, (b) C_3N_4-BiOCl from 350 nm to 600 nm; **c** Photocurrent responses of C_3N_4-BiOCl/ITO electrode for L-cys at different concentration in phosphate buffer; and (**d**) Photocurrent responses of C_3N_4-BiOCl/ITO electrode in phosphate buffer containing L-cys for different concentrations of Cu^{2+}

The photoelectric response capacity of C_3N_4-BiOCl modified ITO electrode for L-cys and Cu^{2+} is then inspected. Figure 1c manifests the typical photocurrents of C_3N_4-BiOCl/PDDA/ITO toward different L-cys concentration. The photocurrents suggest the charge excitation, separation, and transfer in the C_3N_4-BiOCland the response to L-cys. It can be seen in all photocurrent curves, the anodic photocurrent increased with the increase of L-cys levels and the growth

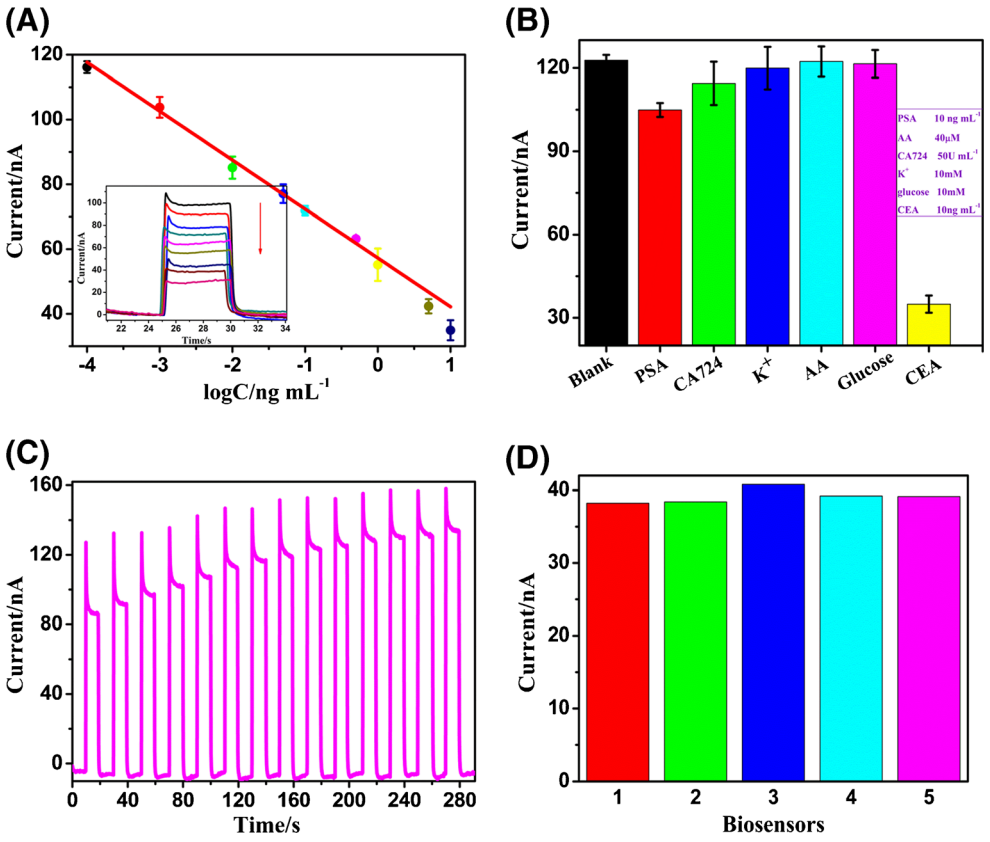

Fig. 2 **a** Calibration plot of the immunoassay toward different concentrations of CEA [*the inset*: photocurrent curves with different CEA concentration at an applied potential of 0 V]; **b** Specificity of photoelectrochemical immunoassay for PSA, AA, CA724, K^+, Glu; **c** Stability of the immunoassay for 300 s; and (**d**) Five groups of immunoassays for 10 ng mL^{-1} CEA detection

Table 1 An overview on recently reported nanomaterial-based methods for determination of CEA

Biomarker	Materials/Methods used	Method applied	Linear range	Detection limit	Reference
CEA	CdTe QDs	Fluorescence	1.0–40.0 ng mL^{-1}	0.3 ng mL^{-1}	[35]
CEA	AuNPs	Liquid crystal	0.001–1 × 10^3 ng mL^{-1}	0.35 pg mL^{-1}	[36]
CEA	Cu_2O/Au nanocomposite	Electrochemical	0.002–20.0 ng mL^{-1}	0.2 pg mL^{-1}	[37]
CEA	Au NPs@ZrHCF@Fe_3O_4	Electrochemical	0.0005–50 ng mL^{-1}	0.15 pg mL^{-1}	[38]
CEA	Hybridization chain reaction	Fluorescent	0.001–2 ng mL^{-1}	0.3 pg mL^{-1}	[39]
CEA	C_3N_4-BiOCl semiconductor	Photoelectrochemical	0.0001–10 ng mL^{-1}	0.1 pg mL^{-1}	This work

tended to balance after 1 mM, indicating the near saturation of the target C_3N_4-BiOCl reaction [32]. In this reaction, L-cys as electron donors was liable to PEC oxidation at current conditions, which can restrain the recombination of e^- and h^+. However, when copper ions are present, L-cysteine as biothiols is a type of chelators, which can capture and coordinate with Cu^{2+} [33]. As shown in Fig. 1d, the anodic photocurrent decreased with the increase of Cu^{2+} concentration. More interestingly, the photocurrent is lower than the blank current of C_3N_4-BiOCl (~60 nA, without L-cys) when the concentration of Cu^{2+} was greater than or equal to 1. The results ascribed to the transfer of photoinduced electrons from the conduction band of the C_3N_4 and BiOCl nanosheets to Cu^{2+} [34]. The mechanisms of PEC toward L-cys and Cu^{2+} are graphically described in Scheme 1b, c. Hence, the L-cys assisted PEC system is sensitive for Cu^{2+}.

Performance of the photoelectrochemical immunoassay

The following parameters were optimized: (a) pH value; (b) incubation time; (c) temperature, and the description and figures are given in the ESM (Fig. S3). Under optimal experimental conditions, sandwich-type immunoassay was constructed on the 96-well microtiter plate for detection a variety of CEA. As shown in Fig. 2a, the photocurrents decreased with the increasing of CEA concentration (*the inset*). The photocurrents were linearly associated with CEA levels in the range of 0.1 pg mL^{-1} ~ 10 ng mL^{-1}. The equation was y (nA) = −15.10 log C (ng mL^{-1}) + 57.27 (R^2 = 0.98, n = 27) with the detection limit (LOD) of 0.1 pg mL^{-1}. On the one hand, since the threshold values in normal human serum is 3 ng mL^{-1} for CEA, this photoelectrochemical immunoassay can completely meet the requirements of clinical diagnosis. For another, an overview on recently reported methods for detection of CEA is listed in the Table 1. Compared with other methods, the immunoassay own wider linear range and lower detection limit. The excellent performance of photoelectrochemical immunoassay mainly attributed to enhanced photoelectric activity of C_3N_4-BiOCl and response capability toward Cu^{2+}. However, the analysis procedures were complicated because the establishment process of immunoassay and detection system of photocurrent was mutually independent. The relationship was built by the function of Cu^{2+}. Therefore, there has been an intense focus on integration in future.

Selectivity, repeatability, and stability of the photoelectrochemical immunoassay

First, ascorbic acid (AA), prostate specific antigen (PSA), carbohydrate antigen 724 (CA724), glucose (Glu), and K^+ were

Table 2 Comparison of the assay results for human serum specimens by using the photoelectrochemical immunoassay and the referenced ELISA method

Sample no.	Found by the PEC immunoassay (mean ± SD%, ng mL^{-1}, n = 3)	Found by ELISA (mean ± SD%, ng mL^{-1}, n = 3)	t_{exp}
1	8.08 ± 2.0	8.19 ± 1.8	−0.87
2	7.12 ± 1.3	7.28 ± 2.2	−1.51
3	6.47 ± 1.2	6.64 ± 1.2	−2.60
4	0.32 ± 0.8	0.31 ± 2.3	2.33
5	1.76 ± 1.3	1.71 ± 2.1	2.06
6	0.06 ± 2.2	–	–
7	0.004 ± 0.5	–	–
8	6.43 ± 2.2	6.91 ± 2.7	−3.52
9	9.19 ± 0.8	9.27 ± 0.7	−1.34
10	0.98 ± 2.0	1.04 ± 1.9	−3.67
11	1.41 ± 2.1	1.35 ± 0.7	3.31

detected by this photoelectrochemical immunoassay. It can be seen in Fig. 2b the value for CEA was lower than that of blank, and values of other substances had no obvious difference with the blank value. As shown in Fig. 2c, the photocurrent of the C_3N_4-BiOCl modified platform for 1 pg mL^{-1} CEA is stability under the repeated light irradiation circles for 280 s. Five groups of immunoassays were built to detect 10 ng mL^{-1} CEA. The variation coefficients (CVs) were 2.58% (Fig. 2d). This immunocomplex was stored in fridge at 4 °C for three weeks, and the photocurrent value reserved 95% compared with initial value. Hence, this photoelectrochemical immunoassay displayed satisfactory selectivity, repeatability, and stability.

Analysis of real serum samples

To verify applicability of photoelectrochemical immunoassay for practical serum samples, *t-test* is employed by contrasting analysis results from photoelectrochemical method and commercial ELISA method. Before experiment, the collected serum samples were handled carefully with dilution by phosphate buffer (pH = 7.0). The experimental results and t_{exp} values are listed in the Table 2. The t_{exp} values in all samples were less than t_{crit} (t_{crit} = 4.30), which declare the immunoassay is believable and possess applicable value in further.

Conclusion

A photoelectrochemical immunoassay for CEA detection was developed by utilizing CuO nanoparticles as labels and cysteine assisted C_3N_4-BiOCl photoelectrochemical system. The heterojunction nanostructure of C_3N_4-BiOC land sacrificial donor of cysteine doubly enhanced the photocurrent response of C_3N_4-BiOCl. The PEC system was sensitive to Cu^{2+} due to its chelation and electron receptors, which doubly decreased the photocurrent response. And Cu^{2+} was introduced from immunoassay format and related to CEA concentrations. Compared with conventional photoelectrochemical detection systems, highlights of this study can be concluded as follows: (i) the background signal of photocurrent was intensive, which was profitable for signal reduction method; (ii) the presence of cysteine improved sensitivity for Cu^{2+}, which was beneficial to immunoassay. This strategy opens a new perspective for the application of photoelectrochemical bioanalysis in the future. Future works should focus on the detection of more biomolecule in serum.

Acknowledgements The National Natural Science Foundation of China (Grant No. 21605111) and Natural Science Foundation of Shanxi Province (No. 201601D021037) are gratefully acknowledged.

Compliance with ethical standards The author(s) declare that they have no competing interests.

References

1. Fang C, Chou C, Yang Y, Wei-Kai T, Wang Y, Chan Y (2018) Multiplexed detection of tumor markers with multicolor polymer dot-based immunochromatography test strip. Anal Chem 90:2134–2140
2. Zhang D, Li W, Ma Z, Han H (2019) Improved ELISA for tumor marker detection using electro-readout-mode based on label triggered degradation of methylene blue. Biosens Bioelectron 126: 800–805
3. Babamiri B, Hallaj R, Salimi A (2018) Ultrasensitive electrochemiluminescence immunoassay for simultaneous determination of CA125 and CA15-3 tumor markers based on PAMAM-sulfanilic acid-$Ru(bpy)_3^{2+}$ and PAMAM-CdTe@CdS nanocomposite. Biosens Bioelectron 99:353–360
4. Zhang K, Lv S, Lu M, Tang D (2018) Photoelectrochemical biosensing of disease marker on p-type cu-doped $Zn_{0.3}Cd_{0.7}S$ based on RCA and exonuclease III amplification. Biosens Bioelectron 117: 590–596
5. Zhang B, Ding C (2016) Displacement-type amperometric immunosensing platform for sensitive determination of tumour markers. Biosens Bioelectron 82:112–118
6. Zheng J, Shen Y, Xu Z, Yuan Z, He Y, Wei C, Er M, Yin J, Chen H (2018) Near-infrared off-on fluorescence probe activated by NTR for in vivo hypoxia imaging. Biosens Bioelectron 119:141–148
7. Shao F, Jiao L, Miao L, Wei Q, Li H (2017) A pH indicator-linked immunosorbent assay following direct amplification strategy for colorimetric detection of protein biomarkers. Biosens Bioelectron 90:1–5
8. Tang J, Xiong P, Cheng Y, Chen Y, Peng S, Zhu Z (2019) Enzymatic oxydate-triggered AgNPs etching: a novel signal-on photoelectrochemical immunosensing platform based on Ag@AgCl nanocubes loaded RGO plasmonic heterostructure. Biosens Bioelectron 130:125–131
9. Tang J, Tang D (2015) Non-enzymatic electrochemical immunoassay using noble metal nanoparticles: a review. Microchim Acta 182: 2077–2089
10. Zhou Q, Xue H, Zhang Y, Lv Y, Li H, Liu S, Shen Y, Zhang Y (2018) Metal-free all-carbon nanohybrid for ultrasensitive photoelectrochemical immunosensing of alpha-fetoprotein. ACS Sensors 3:1385–1391
11. Jung H, Cho K, Kim K, Yoo H, Al-Saggaf A, Gereige I, Jung H (2018) Highly efficient and stable CO_2 reduction photocatalyst with a hierarchical structure of mesoporous TiO_2 on 3D graphene with few-layered MoS_2. ACS Sustain Chem Eng 6:5718–5724
12. Pang F, Zhang R, Lan D, Ge J (2018) Synthesis of magnetite–semiconductor–metal trimer nanoparticles through functional modular assembly: a magnetically separable photocatalyst with photothermic enhancement for water reduction. ACS Appl Mater Interfaces 10:4929–4936
13. Pomilla F, Cortes M, Hamilton J, Molinari R, Barbieri G, Marcì G, Palmisano L, Sharma P, Brown A, Byrne J (2018) An investigation into the stability of graphitic C_3N_4 as a photocatalyst for CO_2 reduction. J Phys Chem C 122:28727–28738
14. Zhao Y, Li R, Mu L, Li C (2017) Significance of crystal morphology controlling in semiconductor-based photocatalysis: a case study on $BiVO_4$ photocatalyst. Cryst Growth Des 17:2923–2928
15. Freitas D, González-Moya J, Soares T, Silva R, Oliveira D, Mansur H, Machado G, Navarro M (2018) Enhanced visible-light photoelectrochemical conversion on TiO_2 nanotubes with Bi_2S_3 quantum dots obtained by in situ electrochemical method. ACS Appl. Energy Mater. 1:3636–3645
16. Hu Y, Huang Y, Wang Z, Wang Y, Ye X, Wong W, Li C, Sun D (2018) Gold/WS_2 nanocomposites fabricated by in-situ ultrasonication and assembling for photoelectrochemical

immunosensing of carcinoembryonic antigen. Microchim Acta 185:570
17. Zhang N, Yang M, Liu S, Sun Y, Xu Y (2015) Waltzing with the versatile platform of graphene to synthesize composite photocatalysts. Chem Rev 115:10307–10377
18. Asahi R, Morikawa T, Irie H, Ohwaki T (2014) Nitrogen-doped titanium dioxide as visible-light-sensitive photocatalyst: designs, developments, and prospects. Chem Rev 114:9824–9852
19. Song K, Ding C, Zhang B, Chang H, Zhao Z, Wei W, Wang J (2018) Dye sensitized photoelectrochemical immunosensor for the tumor marker CEA by using a flower-like 3D architecture prepared from graphene oxide and MoS_2. Microchim Acta 185:310
20. Sun Y, Fan J, Cui L, Ke W, Zheng F, Zhao Y (2019) Fluorometric nanoprobes for simultaneous aptamer-based detection of carcinoembryonic antigen and prostate specific antigen. Microchim Acta 186:152
21. Wang H, Qi C, He W, Wang M, Jiang W, Yin H (2018) A sensitive photoelectrochemical immunoassay of N6-methyladenosine based on dual-signal amplification strategy: Ru doped in SiO_2 nanosphere and carboxylated g-C_3N_4. Biosens Bioelectron 99:281–288
22. Ong W, Tan L, Ng Y, Yong S, Chai S (2016) Graphitic carbon nitride (g-C_3N_4)-based photocatalysts for artificial photosynthesis and environmental remediation: are we a step closer to achieving sustainability. Chem Rev 116:7159–7329
23. Pham T, Shin E (2018) Influence of g-C_3N_4 precursors in g-C_3N_4/$NiTiO_3$ composites on photocatalytic behavior and the interconnection between g-C_3N_4 and $NiTiO_3$. Langmuir 34:13144–13154
24. You Y, Wang S, Xiao K, Ma T, Zhang Y, Huang H (2018) Z-scheme g-C_3N_4/Bi_4NbO_8Cl heterojunction for enhanced photocatalytic hydrogen production. ACS Sustain Chem Eng 6:16219–16227
25. Hua S, Qu D, An L, Jiang W, Wen Y, Wang X, Sun Z (2019) Highly efficient p-type Cu3P/n-type g-C_3N_4 photocatalyst through Z-scheme charge transfer route. Appl Catal B-Environ 240:253–261
26. Mo Z, Xu H, Chen Z, She X, Song Y, Lian J, Zhu X, Yan P, Lei Y, Yuan S, Li H (2019) Construction of MnO_2/monolayer g-C_3N_4 with Mn vacancies for Z-scheme overall water splitting. Appl Catal B Environ 241:452–460
27. Zhong Y, Chen W, Yu S, Xie Z, Wei S, Zhou Y (2018) CdSe quantum dots/g-C_3N_4 heterostructure for efficient H_2 production under visible light irradiation. ACS Omega 3:17762–17769
28. Zhang Y, Xu R, Kang Q, Zhang Y, We Q, Wang Y, Ju H (2018) Ultrasensitive photoelectrochemical biosensing platform for detecting n-terminal pro-brain natriuretic peptide based on SnO_2/SnS_2/mpg-C_3N_4 amplified by PbS/SiO_2. ACS Appl Mater Interfaces 10:31080–31087
29. Manwar N, Chilkalwar A, Nanda K, Chaudhary Y, Subrt J, Rayalu S, Labhsetwar N (2016) Ceria supported Pt/PtO-nanostructures: efficient photocatalyst for sacrificial donor assisted hydrogen generation under visible-NIR light irradiation. ACS Sustain Chem Eng 4:2323–2332
30. Ding C, Song K, Meng H, Zhang B, Zhao Z, Chang H, Wei W (2018) Amplified photoelectrochemical immunoassay for the tumor marker carbohydrate antigen 724 based on dye sensitization of the semiconductor composite C_3N_4-MoS_2. Microchim Acta 185:530
31. Wang Y, Chen L, Liang M, Xu H, Tang S, Yang H, Song H (2017) Sensitive fluorescence immunoassay of alpha-fetoprotein through copper ions modulated growth of quantum dots in-situ. Sensors Actuators B Chem 247:408–413
32. Li Y, Zhang N, Zhao W, Jiang D, Xu J, Chen H (2017) Polymer dots for photoelectrochemical bioanalysis. Anal Chem 89:4945–4950
33. Li F, Liu Y, Zhuang M, Zhang H, Liu X, Cui H (2014) Biothiols as chelators for preparation of N-(aminobutyl)-N-(ethylisoluminol)/Cu^{2+} complexes bifunctionalized gold nanoparticles and sensitive sensing of pyrophosphate ion. ACS Appl Mater Interfaces 6:18104–18111
34. Lv S, Li Y, Zhang K, Lin Z, Tang D (2017) Carbon dots/g-C_3N_4 nanoheterostructures-based signal-generation tags for photoelectrochemical immunoassay of cancer biomarkers coupling with copper nanoclusters. ACS Appl Mater Interfaces 9:38336–38343
35. Chen Y, Guo X, Liu X, Zhang L (2019) Paper-based fluorometric immunodevice with quantum-dot labeled antibodies for simultaneous detection of carcinoembryonic antigen and prostate specific antigen. Microchim Acta 186:112
36. Zhou C, Zi Q, Wang J, Zhao W, Cao Q (2019) Determination of alkaline phosphatase activity and of carcinoembryonic antigen by using a multicolor liquid crystal biosensor based on the controlled growth of silver nanoparticles. Microchim Acta 186:25
37. Qin Z, Xu W, Chen S, Chen J, Qiu J, Li C (2018) Electrochemical immunoassay for the carcinoembryonic antigen based on the use of a glassy carbon electrode modified with an octahedral Cu_2O-gold nanocomposite and staphylococcal protein for signal amplification. Microchim Acta 185:266
38. Liu L, Zhao G, Li Y, Li X, Dong X, Wei Q, Cao W (2018) A voltammetric immunoassay for the carcinoembryonic antigen using a self-assembled magnetic nanocomposite. Microchim Acta 185:387
39. Yang W, Zhou X, Zhao J, Xu W (2018) A cascade amplification strategy of catalytic hairpin assembly and hybridization chain reaction for the sensitive fluorescent assay of the model protein carcinoembryonic antigen. Microchim Acta 185:100